Available online at www.sciencedirect.com
ScienceDirect
J. Chem. Thermodynamics 40 (2008) 193–202
JCT
www.elsevier.com/locate/jct

Kinematic viscosity and speed of sound in gaseous CO, CO_2, SiF_4, SF_6, C_4F_8, and NH_3 from 220 K to 375 K and pressures up to 3.4 MPa

Andrés F. Estrada-Alexanders *,[1], John J. Hurly

Fluid Metrology Group, Process Measurement Division, NIST, Gaithersburg, MD 20899-8360, USA

Received 28 March 2007; received in revised form 29 June 2007; accepted 9 July 2007
Available online 18 July 2007

Abstract

An acoustic Greenspan viscometer was used to measure the kinematic viscosity and speed of sound in the gases: CO, CO_2, SiF_4, SF_6, C_4F_8, and NH_3. The measurements cover the temperature range 220 K to 375 K, and pressures up to 3.4 MPa or 80% of the saturation pressure.

The viscometer was calibrated at 298.16 K using five reference gases, Ar, He, N_2, CH_4, and C_3H_8, for which the viscosity and the speed of sound are known. With this calibration, we estimated the relative standard uncertainty of the kinematic viscosity $u_r(\eta/\rho) = 0.006$ and the uncertainty of speed of sound $u_r(c) = 0.0001$, except for very low pressures where the signal-to-noise ratio deteriorates and quality factor for the Helmholtz mode is $\leqslant 20$.

Keywords: Greenspan viscometer; Kinematic viscosity; Speed of sound; Argon; Helium; Nitrogen; Methane; Propane; Carbon monoxide; Carbon dioxide; Silicon tetrafluoride; Sulfur hexafluoride; Octafluorocyclobutane; Ammonia

1. Introduction

In recent years, there have been advances in experimental techniques for the accurate measurement of a gas viscosity. Some of these elegant experiments are able to measure the viscosity of gases to heretofore unachieved accuracies. Wilhelm and Vogel [1] used a vibrating-wire viscometer reporting an uncertainty of ±0.2% away from the critical point. Evers *et al.* [2] determined both the viscosity and the density by measuring the buoyancy and decay rate of rotations of a magnetically suspended cylinder. They report uncertainties in viscosity below ±0.15% in the dilute gas region and less then ±0.4% at higher densities. Most recently Berg [3] measured the viscosity of helium at 298 K, by modeling gas flow through a long capillary, resulting in an uncertainty of ±0.08%. All three of these methods, while extremely accurate, require great care in operation, and employ delicate instruments. In this paper, we use a complete different technique that is able to determine simultaneously both speed of sound, c and kinematic viscosity, $\nu = \eta/\rho$ in gases with nearly the same accuracy that others have obtained recently.

In 1953, Greenspan and Wimenitz [4] proposed determining the viscosity of a gas by measuring the energy losses in a double Helmholtz acoustic resonator. In the literature, this device is referred to as a Greenspan viscometer, in recognition of their work. Since 1996 several Greenspan viscometers [5–10] have been described. Each of the previous designs has advanced the understanding of Greenspan viscometer and the robust acoustic model based on transmission line equations [8]. This technique for measuring viscosity of a gas has the advantages of: high accuracy over a large temperature range, a robust cell which holds high

* Corresponding author. Permanent address: Departamento de Física, Universidad Autónoma Metropolitana-Iztapalapa, Apdo. Postal 55-534, México, D.F., 09340, Mexico. Tel.: +52 55 5804 4614; fax: +52 55 5804 4611.
E-mail address: afea@xanum.uam.mx (A.F. Estrada-Alexanders).
[1] On sabbatical leave.

0021-9614/$ - see front matter © 2007 Elsevier Ltd. All rights reserved.
doi:10.1016/j.jct.2007.07.002

pressures, and all wetted surfaces are metal allowing the study of reactive gases that might destroy other instruments.

In this paper, we present results of the latest version of the Greenspan viscometer and investigate the end correction impedance term in the acoustic model. In the previous versions of the Greenspan viscometer, the sharp right angle ends of the main duct create weak singularities in the flow field that precluded an exact solution. Thus, the viscometer relied on numerical calculations of the end correction [6]. In order to fit the reference gases to within their claimed uncertainties, empirical corrections were included [5,7–9]. The resonator discussed in this work was fabricated with rounded ends to the main duct and rounded corners of the chamber volumes. These modifications allowed the accurate calculation of an effective-area that took into account thermal surface losses. The localized impedance at the rounded duct ends are described with a lumped-component model such that $Z_{\mathrm{end}} = \rho\omega/[A_{\mathrm{d}}(\mathrm{i}\delta_{\mathrm{I}} + \delta_{\mathrm{R}})]$, where ρ is the density, ω the (angular) frequency, A_{d} the area of the duct, and δ_{I} and δ_{R} are the inertial and resistive lengths, respectively. The inertial and resistive lengths were evaluated numerically and then, they were approximated by simple polynomials of the viscous penetration length, δ_{v} [11].

The following sections describe the new apparatus, its performance, the need for a calibration, and finally experimental values are presented for c and v in CO, CO_2, SiF_4, C_4F_8, NH_3, and SF_6. We report the kinematic viscosity v rather and the shear viscosity, η of these gases because the equations of state for these gases have high uncertainties in predicted values of ρ from the measured variables pressure p and temperature T. In a future paper, we will derive an approximate equation of state based on the speed of sound measurements reported here, from which ρ will be derived permitting the determination of η from the values of v reported here.

2. Apparatus

Figure 1 shows the new Greenspan viscometer, that was constructed out of Monel alloy 400 (approximately 2/3 nickel and 1/3 copper) to provide corrosion resistance. The main duct had a 2.5 mm radius (r_{d}); its ends were rounded with a 2 mm radius. The fill tube had a 0.5 mm radius (r_{f1}), and was 27 mm long (L_{f1}). The fill duct terminated at a hole in the resonator. This hole had been cut with an electronic discharge machine and was positioned in the center of the duct, where a pressure node is located for the Helmholtz resonance. The diaphragms, 1.5 mm thick with a 7 mm radius, were machined into the end plates. These diaphragms were sufficiently thick that the resonator acted as its own pressure vessel. This permitted the resonator to be immersed in the stirred thermostatic bath greatly reducing the time required for the resonator to reach temperature equilibrium. A 6 mm o.d. well was drilled into the center of the resonator to house a standard platinum resistance thermometer for temperature measurements.

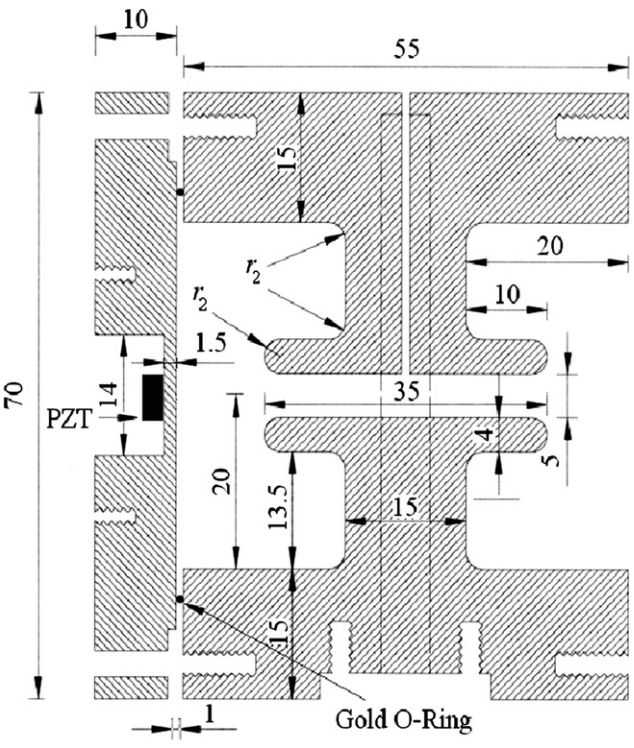

Figure 1. Schematic cross-section of Greenspan viscometer; piezoceramic transducer (PZT) and gold O-ring are shown with arrows; r_2 is the fillet radius with nominal value of 2 mm. All dimensions are in millimeters.

All interior surfaces of the viscometer were polished to a mirror finish. Then the Precision Engineering Division of NIST measured the internal dimensions of the surfaces of the main body of the resonator using a coordinate measurement machine (CMM). This CMM had a resolution of 10^{-5} mm, a repeatability of 10^{-4} mm and an uncertainty of $\pm 5 \cdot 10^{-4}$ mm or better, depending on the properties of the surface under study. From the CMM results, the dimensions of the resonator were determined to be: chamber volume, V_{ch}, 23,691 mm^3, chamber internal surface area, S_{ch}, 5246.4 mm^2, the mean duct radius, r_{d}, 2.5056 mm, duct length, L_{d}, 30.903 mm, all at the temperature of 293.15 K. We considered these values as the nominal dimensions of the resonator. Below, we reviewed these figures in the light of the calibration results obtained with five reference gases (Ar, He, N_2, CH_4, and C_3H_8) at $T = 298.16$ K.

A 3.175 mm o.d. Monel alloy 400 tube, about 500 mm long (L_{f2}), and with about 1 mm i.d. ($2 \cdot r_{\mathrm{f2}}$) was welded to end of the fill tube to connect the resonator to an alloy 400 gas handling manifold by means of a pneumatic valve, with a dead volume of 600 mm^3 (V_{ft}), which closes the resonator and allowed the increase or decrease of the gas pressure. Two 0.25 mm gold O-rings sealed the end plates on the body of the resonator. The end plates were fastened to the resonator body with 12 high-strength 5-40 alloy screws. Thin piezoceramic disks were firmly cemented to the outside surface of each diaphragm with a high temperature epoxy. These transducers generated and detected

sound. The polarization for these disks was oriented perpendicular to the electrodes. A function generator drove the source transducer with a sinusoidal voltage at frequency f, and it provided the reference signal for a digital, two-phase lock-in amplifier. The lock-in amplifier measured the in-phase and quadrature signals, also at f, from the detector transducer.

The resonator was suspended vertically using three one-quarter inch (1/4″) threaded rods, and submerged in a stirred thermostatic bath. The bath liquid was silicon oil for temperatures above room temperature, and methanol below room temperature. The experimental set up and data collection (computer controlled) was identical to that described in reference [9]. Here, we only want to recall that for each acoustic resonance studied, the drive and detector voltages were measured at 22 frequencies spanning twice the half-width, g, of the resonance. The frequency was scanned upward and downward to remove the effects of a linear temperature drift. The measured signal was averaged for 2 s at each frequency.

3. Calibration

The network impedance model that describes the response of an acoustic signal inside the resonator depends primarily upon the physical dimensions of the resonator. The end corrections [8] accounting for the flow field at the ends of the main duct are an important refinement to the model. The dimensions of the resonator are given in table 1, as are the coefficients that describe end corrections as discussed below. The data from the CMM revealed some geometric imperfections of the duct. Its surface was not as smooth as we has expected; the irregularities were about 8 parts per thousand of the nominal radius. However, the main imperfection of the duct was its narrowing near the middle. Thus, instead of using the nominal value of the duct radius, we used an effective radius that we obtained from the average of the coordinate measurements of the radius at different positions along the duct. This procedure reduced the nominal radius from 2.5056 mm to 2.5000 mm. The duct length was obtained from the difference between the total duct length (including the rounded ends) and the curvature radius of each end. This procedure was used because it is difficult to determine where the rounded edge finished and the straight part of the duct starts. Volume and surface of the chambers were obtained from numerical calculations of the idealized cross-section of the resonator. It is important to mention that surface area of the chamber is replaced by and effective-area S_{eff} which describes better the thermal losses in each cavity. This effective surface is obtained by weighting the geometric surface area by the square of the acoustic temperature [11]. This procedure makes that S_{eff} is about 0.9923 times the geometric surface.

Figure 1 shows that each chamber was sealed with a gold O-ring that is connected to the chamber by a rectangular slit with a depth l_s and an annular gap of thickness $2d_s$. After finishing the measurement program of all gases, we opened the resonator and estimated both $l_s \approx 2.3$ mm and $d_s \approx 0.03$ mm as an average of both O-rings. Although these dimensions are small compared with the other dimensions of the resonator, thermal losses are increased by the slits because the thermal penetration length δ_t is of the order of d_s, for most of the experimental conditions. Therefore, we included in our model a correction to take into account this effect with the appropriate formula for this particular slit geometry [12].

Previous resonators suffered from a partial knowledge of the end corrections, and therefore calibrations were needed. In the particular design of our resonator, all edges inside the cavity were rounded, because under this configuration, excessive thermal losses due to sharp corners were avoided and also because it was possible to calculate numerically, both δ_R and δ_I. These quantities were approximated as polynomials of the ratio of $\varepsilon_v \equiv \delta_v/r_d$, whose coefficients depend on the specific dimensions of the resonator. We had expressions of these polynomials from numerical calculations [11],

$$\begin{aligned} \delta_I &\approx r_d(1.1694 + 1.083\varepsilon_v + 14.6\varepsilon_v^2 + 20\varepsilon_v^3), \\ \delta_R &\approx \delta_v(1.0871 + 1.354\varepsilon_v + 0.75\varepsilon_v^2), \end{aligned} \tag{1}$$

but they were obtained assuming no imperfections in geometry neither a slit correction due to the gold seal. Thus, they did not give us the expected viscosity; the deviations were as large as ±1.7% from the reference values of the viscosity. Furthermore, the values of speed of sound were systematically larger than reference speeds of sound c_{ref}; $\delta c \equiv c - c_{\text{ref}}$ varied linearly with ε_v. Perhaps small asymmetries between each chamber (which so far have been assumed to be identical) arising from different rounded end radius and different actual slit dimensions in each chamber produce slightly different coefficients for the polynomials δ_R and δ_I, however, the polynomial forms should be satisfactory. The polynomial coefficients were obtained from a fit of five reference gases with known viscosity at the temperature of 298.16 K. These coefficients are given in table 1 and the average absolute deviation of 80 points used for this calibration was about of 0.3%. Except

TABLE 1
Final parameters used in the network impedance model

Parameter	Value	Parameter	Value	Parameter	Value
V_{ch}/m^3	$2.3691 \cdot 10^{-5}$	L_{f2}/m	$5.0 \cdot 10^{-1}$	$\varepsilon_{i,0}$	1.17911
S_{eff_ch}/m^2	$5.24638 \cdot 10^{-3}$	V_{ft}/m^3	$6.0 \cdot 10^{-7}$	$\varepsilon_{i,1}$	0.840989
r_d/m	$2.500 \cdot 10^{-3}$	d_s/m	$3.0 \cdot 10^{-5}$	$\varepsilon_{i,2}$	5.13551
L_d/m	$3.0944 \cdot 10^{-2}$	l_s/m	$2.3 \cdot 10^{-3}$	$\varepsilon_{i,3}$	8.37010
r_{f1}/m	$5.33 \cdot 10^{-4}$			$\varepsilon_{r,0}$	1.12667
L_{f1}/m	$2.75 \cdot 10^{-2}$			$\varepsilon_{r,1}$	0.710053
r_{f2}/m	$8.4 \cdot 10^{-4}$			$\varepsilon_{r,2}$	−0.949563

All dimensions are determined at 293.15 K, and end correction coefficients, $\varepsilon_{i,m}$ and $\varepsilon_{r,n}$ with $m = 0,1,2,3$ and $n = 0,1,2$ for (δ_I/r_d) and (δ_R/δ_v), respectively, were obtained from fittings of the five reference gases at 298.16 K. Subscript m (or n) corresponds to the power $(\varepsilon_v)^m$.

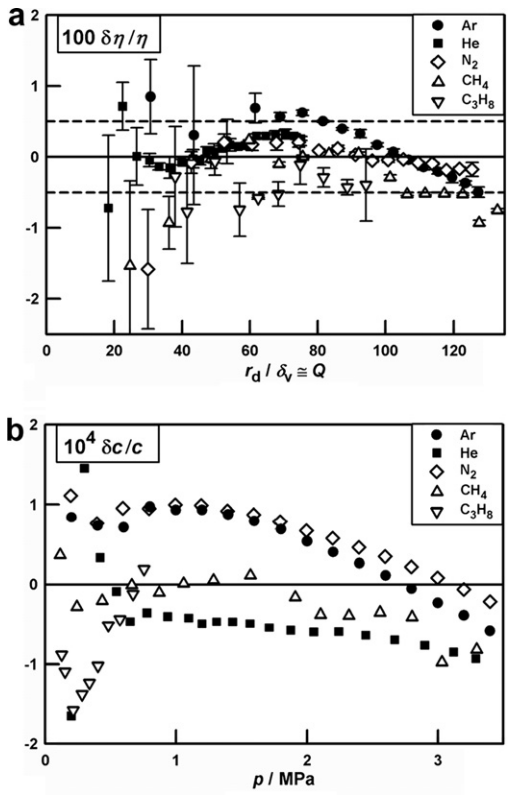

Figure 2. Calibration of the Greenspan viscometer using five reference gases to obtain the end correction coefficients at 298.16 K. (a) Relative deviations of viscosity $(\eta - \eta_{ref})/\eta_{ref} \equiv \delta\eta/\eta$ as function of $r_d/\delta_v \approx Q$; Ar, ●, reference [1]; He, ■, reference [14]; N_2, ◇, reference [15]; CH_4, △, reference [16]; C_3H_8, ▽, reference [17]. Error bars are one standard deviation, and dotted line represents ±0.5%. (b) Relative deviations of speed of sound $\delta c/c$ as function of p; Ar, ●, reference [13]; He, ■, reference [14]; N_2, ◇, reference [18]; CH_4, △, reference [19]; C_3H_8, ▽, reference [20].

for one point of nitrogen and few points of methane, the difference between the reference and the fitted viscosity was within ±0.5%, as can be seen in figure 2a. This fitting reduced the end corrections by a factor of three with respect to equation (1). In figure 2b, we plotted the deviations of the speed of sound in these five gases after calibration; the agreement is now within ±0.01% for most pressures.

4. Analysis and results

Kinematic viscosity and speed of sound were determined from the measured resonance of Helmholtz mode for each of the following substances in the gaseous phase: carbon monoxide (CO), carbon dioxide (CO_2), ammonia (NH_3), octafluorocyclobutane (C_4F_8), tetrafluorosilane (SiF_4), and sulfur hexafluoride (SF_6). For all these substances, the in-phase U and quadrature V voltage signals were fitted simultaneously to the completed network model given in reference [8] by means of a non-linear fitting routine. This model related the complex voltage $W = U + iV$ to the equivalent impedance Z_{eq} by means of a proportional constant (equation (36) of reference [8]); some background terms are normally needed to fit the resonance pattern within ±0.02% of the maximum voltage amplitude.

For almost all resonances, an 8-parameter fit (three complex coefficients, v and c) was satisfactory. The initial guess for v and c was obtained from rough correlations based on corresponding states or from published databases [21], while for the three complex coefficients the initial guess was obtained from a fitting of the experimental data to a simpler approximate expression as

$$U + iV = \frac{ifA}{f^2 - (f_0 + ig)^2} + B + C\Delta f, \qquad (2)$$

where A, B and C, are complex coefficients, f_0 and g are the resonance frequency and half-width respectively, and $\Delta f = f - \tilde{f}$, where $\tilde{f}$ is a constant frequency near the middle of the frequency range swept. In some cases, at low densities the inclusion of a quadratic term in Δf as background in equation (2) was needed so a 10-parameter fit was used to achieve the same quality-of-fit as the rest of the data.

Except for SF_6, several isotherms were measured for each gas; at temperatures below the critical temperature, we restricted the maximum pressure to be ⩽80% of the corresponding saturation pressure. At supercritical temperatures, the maximum pressure used was smaller of the cylinder sample pressure of each gas or the pressure of 3.4 MPa. Temperature control was better than ±0.01 K, and pressure stability was within ±0.01 kPa. Thus, the contribution of uncertainty in p and T to the final uncertainty budget for both the speed of sound and the kinematic viscosity can be neglected.

Small thermal expansion corrections to the resonator dimensions were applied to take into account temperature difference from T with the reference temperature ($T = 293.15$ K) at which the CCM measured the resonator's geometry.

For all T and p, four scans around the resonance frequency were performed and analyzed with the network model; in only 15 out of 77 state points of SiF_4, the analysis included three scans instead of the original four scans. Only three out of 433 total state points measured with the resonator were discarded for showing inconsistencies. In tables 2 to 7, we reported the fitted value of 430 state points, after averaging the results of the four (or three) scans in each T and p. The uncertainty associated to v and c is one standard deviation.

Normally, the uncertainty of v was about $5 \cdot 10^{-9}$ m^2/s except for pressures of the order of 500 kPa were this figure increased by up to $3 \cdot 10^{-8}$ m^2/s. At pressures below 500 kPa, quality factors became smaller ($Q \leqslant 30$) and then precision of v deteriorated rapidly with pressure decreases. At isolated state points, where the resonance frequency of the Helmholtz mode was a multiple of 60 Hz, the electrical pickup reduced the signal-to-noise ratio reducing the precision of v.

For c the situation is similar; the precision of c was about few parts per ten thousand for almost all state points; for only few low pressure measurements the precision was a factor of ten worse. We stress that this level

TABLE 2
Kinematic viscosity v and speed of sound c of CO at different temperatures

T/K	p/kPa	$10^6 v/(m^2/s)$	c/(m/s)
225.00	2000.00	0.4659 ± 0.0042	304.940 ± 0.010
	1750.00	0.5317 ± 0.0013	304.952 ± 0.006
	1500.00	0.6194 ± 0.0034	304.987 ± 0.005
	1250.00	0.7365 ± 0.0064	305.043 ± 0.016
	1000.00	0.9402 ± 0.0036	305.154 ± 0.003
	750.00	1.2332 ± 0.0093	305.259 ± 0.012
	499.99	1.858 ± 0.025	305.400 ± 0.015
	250.04	3.742 ± 0.022	305.594 ± 0.045
225.00	2454.70	0.3787 ± 0.0025	304.965 ± 0.003
	2263.97	0.4141 ± 0.0021	304.936 ± 0.008
	2016.09	0.4629 ± 0.0020	304.908 ± 0.005
	1787.07	0.5204 ± 0.0033	304.910 ± 0.004
	1581.46	0.5882 ± 0.0032	304.937 ± 0.009
	1345.57	0.6952 ± 0.0025	304.994 ± 0.004
	1141.55	0.8167 ± 0.0034	305.059 ± 0.007
	934.61	1.0005 ± 0.0037	305.141 ± 0.004
	743.07	1.2530 ± 0.0048	305.237 ± 0.007
	560.56	1.675 ± 0.030	305.344 ± 0.013
	371.90	2.502 ± 0.094	305.415 ± 0.057
250.00	2241.48	0.5084 ± 0.0014	323.445 ± 0.004
	2050.14	0.5565 ± 0.0034	323.271 ± 0.006
	1808.18	0.6278 ± 0.0035	323.080 ± 0.011
	1587.81	0.7193 ± 0.0052	322.926 ± 0.009
	1392.31	0.8191 ± 0.0022	322.794 ± 0.004
	1169.11	0.9777 ± 0.0072	322.667 ± 0.017
	982.55	1.163 ± 0.012	322.583 ± 0.008
	791.25	1.4462 ± 0.0080	322.506 ± 0.015
	587.83	1.955 ± 0.022	322.431 ± 0.038
	401.55	2.878 ± 0.033	322.400 ± 0.058
	221.65	5.37 ± 0.36	322.56 ± 0.42
275.00	2000.00	0.6961 ± 0.0026	340.229 ± 0.004
	1750.00	0.7885 ± 0.0041	339.887 ± 0.005
	1500.00	0.920 ± 0.011	339.570 ± 0.013
	1250.00	1.109 ± 0.021	339.265 ± 0.034
	1000.00	1.371 ± 0.028	338.987 ± 0.035
	750.00	1.840 ± 0.071	338.756 ± 0.056
	500.41	2.70 ± 0.05	338.478 ± 0.035
	250.64	5.04 ± 0.53	338.34 ± 0.38
275.00	2364.73	0.5787 ± 0.0023	340.694 ± 0.011
	2150.85	0.6334 ± 0.0015	340.383 ± 0.006
	1882.65	0.7231 ± 0.0006	340.017 ± 0.006
	1675.00	0.8124 ± 0.0025	339.741 ± 0.006
	1443.14	0.9450 ± 0.0051	339.459 ± 0.003
	1252.24	1.0859 ± 0.0096	339.219 ± 0.010
	1045.38	1.297 ± 0.011	338.985 ± 0.009
	832.04	1.6325 ± 0.0099	338.755 ± 0.008
	652.16	2.0691 ± 0.0066	338.540 ± 0.017
	465.90	2.827 ± 0.048	338.322 ± 0.069
	286.53	4.39 ± 0.14	338.19 ± 0.11
300.00	2000.00	0.8319 ± 0.0042	356.146 ± 0.019
	1750.00	0.9467 ± 0.0015	355.741 ± 0.002
	1500.00	1.0997 ± 0.0035	355.324 ± 0.006
	1250.01	1.3138 ± 0.0017	354.914 ± 0.005
	1000.01	1.6371 ± 0.0048	354.517 ± 0.012
	709.53	2.28 ± 0.24	354.00 ± 0.12
	501.19	3.248 ± 0.022	353.744 ± 0.022
	252.56	6.71 ± 0.12	353.435 ± 0.082
300.00	2005.34	0.8272 ± 0.0011	356.146 ± 0.003
	1868.03	0.8890 ± 0.0009	355.910 ± 0.004
	1730.28	0.9548 ± 0.0028	355.674 ± 0.001
	1602.13	1.0286 ± 0.0030	355.460 ± 0.002
	1481.47	1.1191 ± 0.0051	355.267 ± 0.005
	1373.95	1.2005 ± 0.0046	355.091 ± 0.009
	1178.09	1.3919 ± 0.0031	354.777 ± 0.003
325.00	2413.09	0.7660 ± 0.0049	371.819 ± 0.008
	2129.59	0.8627 ± 0.0044	371.218 ± 0.009
	1908.67	0.9623 ± 0.0027	370.769 ± 0.007
	1633.88	1.1232 ± 0.0039	370.218 ± 0.006
	1401.15	1.3120 ± 0.0030	369.773 ± 0.002
	1169.67	1.5703 ± 0.0073	369.334 ± 0.011
	943.23	1.9423 ± 0.0035	368.907 ± 0.008
	732.01	2.486 ± 0.016	368.516 ± 0.008
	515.56	3.492 ± 0.048	368.109 ± 0.044
	303.08	5.93 ± 0.18	367.794 ± 0.069
350.00	2464.21	0.8552 ± 0.0006	386.207 ± 0.003
	2208.19	0.9512 ± 0.0016	385.622 ± 0.004
	1995.63	1.0517 ± 0.0065	385.142 ± 0.005
	1735.08	1.2073 ± 0.0085	384.562 ± 0.014
	1461.54	1.4283 ± 0.0053	383.965 ± 0.004
	1245.13	1.6838 ± 0.0074	383.511 ± 0.007
	1007.12	2.0632 ± 0.0073	382.991 ± 0.013
	775.52	2.693 ± 0.017	382.518 ± 0.010
	544.10	3.842 ± 0.032	382.059 ± 0.012
	342.40	6.04 ± 0.13	381.628 ± 0.062
375.00	2518.19	0.9404 ± 0.0037	399.799 ± 0.004
	2250.59	1.0486 ± 0.0026	399.115 ± 0.002
	2026.16	1.1640 ± 0.0036	398.558 ± 0.005
	1815.58	1.2955 ± 0.0018	398.035 ± 0.003
	1537.48	1.5266 ± 0.0058	397.369 ± 0.002
	1302.30	1.8071 ± 0.0067	396.823 ± 0.003
	1102.86	2.129 ± 0.011	396.344 ± 0.008
	885.97	2.6282 ± 0.0087	395.844 ± 0.010
	672.43	3.418 ± 0.040	395.315 ± 0.012
	460.71	4.992 ± 0.085	394.79 ± 0.11
	260.28	8.45 ± 0.59	394.36 ± 0.22

of precision in c is acceptable because the Helmholtz mode has a quality factor of one hundred or less, by design. This is two orders of magnitude lower than the quality factor of a spherical resonator used for measuring speed of sound in gases to the highest possible precision [13].

In some substances, one repetition of an isotherm was performed to check reproducibility with a fresh gas sample. This test provided evidence that the test gas was stable within the resonator at that it did not become progressively contaminated. The repeated isotherms are shown in the tables in the order that they were taken. In all cases, a satisfactory reproducibility was achieved, and no abrupt changes in v were observed between repetitions, as figure 3 shows for CO at 300 K.

We also did some measurements in Ar, which ρ is quite well known, so we were able to derive straightforward η from v and compare with values reported in the literature [1]. Figure 4 shows this comparison; also it is shown, a comparison of c obtained from our viscometer with values

TABLE 3
Kinematic viscosity v and speed of sound c of CO_2 at different temperatures

T/K	p/kPa	$10^6 v/(m^2/s)$	c/(m/s)
220.00	479.78	0.9019 ± 0.0031	225.763 ± 0.008
	449.74	0.9699 ± 0.0014	226.424 ± 0.010
	425.51	1.0287 ± 0.0019	226.947 ± 0.002
	393.15	1.1195 ± 0.0068	227.642 ± 0.007
	362.71	1.225 ± 0.013	228.286 ± 0.011
	324.47	1.3750 ± 0.0074	229.072 ± 0.005
	288.21	1.5567 ± 0.0067	229.811 ± 0.010
	254.44	1.7918 ± 0.0098	230.535 ± 0.011
	226.71	2.003 ± 0.012	231.053 ± 0.006
	195.46	2.367 ± 0.033	231.697 ± 0.020
235.00	803.31	0.5951 ± 0.0049	228.810 ± 0.008
	723.88	0.6708 ± 0.0025	230.307 ± 0.007
	638.46	0.7665 ± 0.0029	231.866 ± 0.005
	545.18	0.9134 ± 0.0015	233.524 ± 0.004
	452.88	1.1143 ± 0.0019	235.117 ± 0.002
	359.42	1.4232 ± 0.0022	236.686 ± 0.003
	224.78	2.312 ± 0.013	238.870 ± 0.008
250.00	1438.24	0.3544 ± 0.0009	227.814 ± 0.001
	1291.60	0.4031 ± 0.0015	230.374 ± 0.005
	1177.57	0.4497 ± 0.0004	232.284 ± 0.001
	1060.25	0.5065 ± 0.0009	234.183 ± 0.003
	953.03	0.5715 ± 0.0009	235.866 ± 0.002
	818.89	0.6754 ± 0.0005	237.904 ± 0.001
	702.28	0.7985 ± 0.0005	239.622 ± 0.000
	595.84	0.9534 ± 0.0008	241.151 ± 0.001
	491.25	1.1702 ± 0.0003	242.616 ± 0.003
	372.33	1.5676 ± 0.0019	244.249 ± 0.002
	274.20	2.1534 ± 0.0070	245.572 ± 0.007
270.00	2509.61	0.2258 ± 0.0021	226.693 ± 0.004
	2316.11	0.2494 ± 0.0011	229.714 ± 0.002
	2079.64	0.2837 ± 0.0004	233.186 ± 0.003
	1846.01	0.3262 ± 0.0009	236.431 ± 0.003
	1630.02	0.3763 ± 0.0008	239.286 ± 0.004
	1446.70	0.4309 ± 0.0004	241.616 ± 0.003
	1287.09	0.4911 ± 0.0008	243.582 ± 0.002
	1076.54	0.5989 ± 0.0007	246.097 ± 0.002
	898.25	0.7277 ± 0.0022	248.157 ± 0.003
	705.02	0.9474 ± 0.0031	250.332 ± 0.001
	526.01	1.2881 ± 0.0066	252.297 ± 0.009
	354.95	1.953 ± 0.048	254.132 ± 0.047
	196.61	3.504 ± 0.061	255.766 ± 0.062
285.00	3057.76	0.2062 ± 0.0010	232.506 ± 0.004
	2841.89	0.2271 ± 0.0007	235.226 ± 0.000
	2559.66	0.2576 ± 0.0008	238.616 ± 0.001
	2221.25	0.3032 ± 0.0005	242.477 ± 0.002
	1947.24	0.3524 ± 0.0003	245.461 ± 0.002
	1707.23	0.4086 ± 0.0001	247.983 ± 0.002
	1500.40	0.4716 ± 0.0003	250.092 ± 0.001
	1228.51	0.5874 ± 0.0005	252.793 ± 0.002
	1012.98	0.7217 ± 0.0009	254.874 ± 0.001
	787.74	0.9437 ± 0.0022	257.000 ± 0.001
	575.25	1.3113 ± 0.0028	258.960 ± 0.003
	371.48	2.0695 ± 0.0082	260.813 ± 0.009
300.00	3145.79	0.2334 ± 0.0004	243.815 ± 0.001
	2893.94	0.2570 ± 0.0010	246.209 ± 0.002
	2577.86	0.2916 ± 0.0006	249.121 ± 0.001
	2272.21	0.3370 ± 0.0004	251.857 ± 0.002
	1991.46	0.3899 ± 0.0001	254.302 ± 0.001
	1747.76	0.4502 ± 0.0004	256.377 ± 0.001
	1526.14	0.5216 ± 0.0003	258.228 ± 0.001
	1237.01	0.6539 ± 0.0006	260.596 ± 0.001
	993.26	0.8257 ± 0.0006	262.550 ± 0.001
	748.54	1.1095 ± 0.0006	264.479 ± 0.001
	531.89	1.5815 ± 0.0015	266.161 ± 0.001
	313.43	2.7182 ± 0.0048	267.831 ± 0.003
304.77	3135.88	0.2441 ± 0.0013	247.426 ± 0.002
	2881.02	0.2686 ± 0.0020	249.657 ± 0.003
	2552.72	0.3072 ± 0.0008	252.452 ± 0.001
	2235.18	0.3566 ± 0.0005	255.087 ± 0.001
	1949.98	0.4142 ± 0.0004	257.402 ± 0.003
	1699.38	0.4816 ± 0.0002	259.398 ± 0.002
	1478.86	0.5593 ± 0.0002	261.121 ± 0.001
	1201.73	0.6981 ± 0.0008	263.256 ± 0.001
	979.77	0.8661 ± 0.0008	264.938 ± 0.001
	745.25	1.1528 ± 0.0008	266.692 ± 0.001
	527.05	1.6498 ± 0.0030	268.300 ± 0.003
	317.81	2.782 ± 0.013	269.839 ± 0.009
310.00	3077.99	0.2605 ± 0.0011	251.560 ± 0.003
	2708.78	0.3003 ± 0.0005	254.502 ± 0.001
	2362.96	0.3494 ± 0.0006	257.194 ± 0.002
	2055.58	0.4075 ± 0.0002	259.537 ± 0.001
	1786.58	0.4745 ± 0.0002	261.551 ± 0.001
	1549.04	0.5533 ± 0.0001	263.303 ± 0.002
	1259.27	0.6896 ± 0.0004	265.404 ± 0.001
	1018.04	0.8635 ± 0.0007	267.131 ± 0.001
	773.76	1.1495 ± 0.0009	268.857 ± 0.001
	552.05	1.6300 ± 0.0001	270.405 ± 0.001
	342.08	2.661 ± 0.012	271.862 ± 0.009
330.00	3067.62	0.3059 ± 0.0013	264.214 ± 0.002
	2778.74	0.3396 ± 0.0005	265.942 ± 0.001
	2423.40	0.3943 ± 0.0009	268.057 ± 0.003
	2103.20	0.4586 ± 0.0010	269.943 ± 0.003
	1813.09	0.5371 ± 0.0004	271.644 ± 0.001
	1559.26	0.6298 ± 0.0004	273.117 ± 0.000
	1332.98	0.7428 ± 0.0006	274.426 ± 0.001
	1059.35	0.9444 ± 0.0004	275.997 ± 0.001
	846.53	1.1907 ± 0.0007	277.211 ± 0.000
	626.86	1.6211 ± 0.0012	278.458 ± 0.002
	402.42	2.5505 ± 0.0023	279.728 ± 0.003
	201.27	5.168 ± 0.014	280.886 ± 0.004
350.00	3133.84	0.3421 ± 0.0016	275.009 ± 0.002
	2827.17	0.3819 ± 0.0004	276.429 ± 0.001
	2447.32	0.4451 ± 0.0004	278.194 ± 0.001
	2228.51	0.4920 ± 0.0005	279.211 ± 0.001
	1872.95	0.5901 ± 0.0004	280.864 ± 0.001
	1584.41	0.7026 ± 0.0003	282.204 ± 0.001
	1347.77	0.8312 ± 0.0004	283.305 ± 0.001
	1143.54	0.9856 ± 0.0014	284.253 ± 0.001
	905.02	1.2532 ± 0.0010	285.360 ± 0.002
	660.10	1.7308 ± 0.0024	286.496 ± 0.002
	440.84	2.6127 ± 0.0052	287.515 ± 0.005
	234.16	4.971 ± 0.032	288.494 ± 0.026
370.00	3095.89	0.3934 ± 0.0006	285.315 ± 0.001
	2771.65	0.4422 ± 0.0009	286.495 ± 0.002
	2382.70	0.5179 ± 0.0004	287.927 ± 0.001
	2019.04	0.6149 ± 0.0008	289.275 ± 0.001
	1714.08	0.7288 ± 0.0009	290.415 ± 0.002

TABLE 3 (*continued*)

T/K	p/kPa	$10^6 v/(m^2/s)$	c/(m/s)
	1449.30	0.8665 ± 0.0008	291.407 ± 0.002
	1228.54	1.0256 ± 0.0011	292.239 ± 0.002
	964.83	1.3150 ± 0.0018	293.237 ± 0.002
	749.31	1.6966 ± 0.0021	294.053 ± 0.002
	537.70	2.3746 ± 0.0085	294.855 ± 0.009
	335.49	3.823 ± 0.018	295.629 ± 0.004

TABLE 4
Kinematic viscosity v and speed of sound c of NH_3 at different temperatures

T/K	p/kPa	$10^6 v/(m^2/s)$	c/(m/s)
300.00	802.82	1.6954 ± 0.0017	413.377 ± 0.001
	676.75	2.0302 ± 0.0072	417.605 ± 0.005
	568.68	2.4461 ± 0.0031	421.025 ± 0.007
	447.86	3.137 ± 0.014	424.670 ± 0.012
	329.51	4.320 ± 0.023	428.067 ± 0.020
	223.53	6.475 ± 0.070	430.996 ± 0.053
300.00	802.37	1.713 ± 0.013	413.013 ± 0.017
	692.80	1.977 ± 0.028	416.702 ± 0.015
	569.79	2.453 ± 0.022	420.632 ± 0.011
	465.77	3.019 ± 0.027	423.726 ± 0.022
	361.99	3.950 ± 0.036	426.770 ± 0.023
	259.87	5.47 ± 0.16	429.552 ± 0.098
315.00	1284.99	1.1321 ± 0.0015	414.392 ± 0.005
	1080.91	1.3636 ± 0.0024	420.458 ± 0.005
	938.74	1.5933 ± 0.0031	424.426 ± 0.003
	791.02	1.9168 ± 0.0031	428.351 ± 0.003
	661.04	2.3351 ± 0.0073	431.685 ± 0.007
	506.43	3.0826 ± 0.0059	435.457 ± 0.008
	378.83	4.193 ± 0.034	438.522 ± 0.019
	250.83	6.409 ± 0.039	441.419 ± 0.036
330.00	1945.84	0.7907 ± 0.0014	413.283 ± 0.010
	1792.05	0.8659 ± 0.0003	417.518 ± 0.007
	1640.80	0.9572 ± 0.0006	421.500 ± 0.003
	1480.49	1.0768 ± 0.0014	425.535 ± 0.003
	1294.82	1.2526 ± 0.0021	430.009 ± 0.004
	1142.12	1.4396 ± 0.0006	433.538 ± 0.002
	977.41	1.7093 ± 0.0034	437.208 ± 0.004
	822.59	2.0604 ± 0.0032	440.539 ± 0.005
	664.29	2.5831 ± 0.0060	443.842 ± 0.006
	473.84	3.685 ± 0.018	447.677 ± 0.016
	308.27	5.766 ± 0.073	450.904 ± 0.029
345.00	2769.00	0.5836 ± 0.0006	411.451 ± 0.003
	2530.02	0.6496 ± 0.0005	417.457 ± 0.006
	2315.57	0.7212 ± 0.0003	422.554 ± 0.003
	1955.14	0.8795 ± 0.0005	430.584 ± 0.002
	1744.59	1.0035 ± 0.0008	435.007 ± 0.003
	1537.04	1.1587 ± 0.0004	439.192 ± 0.002
	1332.13	1.3587 ± 0.0013	443.168 ± 0.003
	1123.20	1.6371 ± 0.0018	447.090 ± 0.005
	914.14	2.0446 ± 0.0022	450.883 ± 0.004
	708.88	2.6651 ± 0.0057	454.468 ± 0.006
	504.54	3.7840 ± 0.0070	457.908 ± 0.014
	297.74	6.499 ± 0.022	461.308 ± 0.016
360.00	3365.40	0.5189 ± 0.0002	418.300 ± 0.004
	3050.47	0.5850 ± 0.0004	424.968 ± 0.004
	2738.78	0.6662 ± 0.0003	431.196 ± 0.009
	2480.70	0.7488 ± 0.0007	436.098 ± 0.002

TABLE 4 (*continued*)

T/K	p/kPa	$10^6 v/(m^2/s)$	c/(m/s)
	2277.38	0.8277 ± 0.0006	439.831 ± 0.005
	1894.78	1.0216 ± 0.0008	446.529 ± 0.004
	1690.65	1.1597 ± 0.0012	449.969 ± 0.003
	1481.15	1.3395 ± 0.0020	453.385 ± 0.003
	1277.79	1.5735 ± 0.0020	456.617 ± 0.003
	1069.66	1.9034 ± 0.0028	459.837 ± 0.002
	865.15	2.3862 ± 0.0076	462.911 ± 0.005
	661.35	3.164 ± 0.018	465.910 ± 0.013
	453.28	4.681 ± 0.041	468.856 ± 0.043
	242.70	8.737 ± 0.048	471.706 ± 0.033
375.00	3379.20	0.5876 ± 0.0045	436.744 ± 0.009
	3140.48	0.6381 ± 0.0041	440.693 ± 0.010
	2933.13	0.6898 ± 0.0032	444.037 ± 0.009
	2599.92	0.7938 ± 0.0060	449.234 ± 0.007
	2290.42	0.9117 ± 0.0013	453.865 ± 0.002
	2026.26	1.0365 ± 0.0071	457.698 ± 0.011
	1793.43	1.2003 ± 0.0098	461.010 ± 0.031
	1583.75	1.3698 ± 0.0080	463.889 ± 0.003
	1341.71	1.634 ± 0.021	467.142 ± 0.031
	1130.68	1.956 ± 0.034	469.931 ± 0.060
	897.66	2.568 ± 0.030	473.000 ± 0.079
	684.74	3.42 ± 0.11	475.646 ± 0.094
	483.31	4.90 ± 0.40	478.26 ± 0.20
	260.57	10.1 ± 1.9	480.64 ± 0.74

TABLE 5
Kinematic viscosity v and speed of sound c of SiF_4 at different temperatures

T/K	p/kPa	$10^6 v/(m^2/s)$	c/(m/s)
215.00	746.64	0.2590 ± 0.0008	125.064 ± 0.006
	649.39	0.3031 ± 0.0007	127.458 ± 0.001
	551.52	0.3602 ± 0.0029	129.725 ± 0.006
	461.43	0.437 ± 0.012	131.701 ± 0.006
	378.50	0.524 ± 0.015	133.422 ± 0.013
	283.66	0.7320 ± 0.0095	135.345 ± 0.022
	198.15	1.056 ± 0.040	136.985 ± 0.050
230.00	1250.99	0.1758 ± 0.0042	122.679 ± 0.009
	1088.35	0.29 ± 0.17	126.351 ± 0.078
	897.83	0.2499 ± 0.0030	130.185 ± 0.012
	742.99	0.2835 ± 0.0069	133.070 ± 0.021
	578.31	0.3985 ± 0.0041	136.010 ± 0.006
	424.62	0.563 ± 0.022	138.593 ± 0.016
	271.49	0.888 ± 0.032	141.023 ± 0.016
245.00	1958.48	0.1246 ± 0.0008	119.337 ± 0.017
	1777.83	0.1399 ± 0.0011	123.040 ± 0.018
	1599.80	0.1551 ± 0.0017	126.373 ± 0.011
	1434.33	0.1738 ± 0.0020	129.263 ± 0.008
	1220.05	0.2078 ± 0.0027	132.777 ± 0.013
	1034.47	0.2457 ± 0.0012	135.635 ± 0.009
	873.41	0.2949 ± 0.0014	138.003 ± 0.006
	703.75	0.3695 ± 0.0084	140.391 ± 0.004
	542.46	0.492 ± 0.012	142.594 ± 0.016
	393.67	0.6602 ± 0.0091	144.547 ± 0.016
	248.32	1.093 ± 0.048	146.400 ± 0.048
260.00	2541.67	0.1097 ± 0.0025	122.510 ± 0.020
	2282.25	0.1247 ± 0.0020	126.449 ± 0.004
	2026.63	0.1392 ± 0.0043	130.083 ± 0.040
	1794.29	0.1575 ± 0.0013	133.230 ± 0.015
	1498.23	0.1911 ± 0.0014	137.011 ± 0.014

(*continued on next page*)

TABLE 5 (*continued*)

T/K	p/kPa	$10^6 v$/(m^2/s)	c/(m/s)
	1252.04	0.2299 ± 0.0032	140.009 ± 0.009
	1047.12	0.2741 ± 0.0065	142.414 ± 0.013
	830.76	0.3543 ± 0.0011	144.876 ± 0.002
	617.98	0.482 ± 0.013	147.215 ± 0.012
	410.06	0.749 ± 0.026	149.455 ± 0.024
	206.14	1.338 ± 0.072	151.460 ± 0.072
274.58	2951.29	0.1076 ± 0.0003	129.468 ± 0.015
	2776.62	0.1150 ± 0.0009	131.328 ± 0.011
	2474.02	0.1305 ± 0.0013	134.503 ± 0.008
	2354.11	0.1361 ± 0.0010	135.736 ± 0.007
	2244.21	0.1424 ± 0.0011	136.847 ± 0.009
	2141.86	0.1518 ± 0.0024	137.920 ± 0.008
	1998.50	0.1639 ± 0.0038	139.335 ± 0.014
	1878.13	0.1704 ± 0.0048	140.505 ± 0.012
	1764.42	0.1819 ± 0.0038	141.624 ± 0.004
	1657.90	0.2006 ± 0.0048	142.673 ± 0.007
	1556.05	0.2093 ± 0.0030	143.641 ± 0.007
	1454.61	0.2279 ± 0.0037	144.620 ± 0.010
	1353.82	0.2422 ± 0.0076	145.573 ± 0.017
	1252.18	0.2594 ± 0.0034	146.525 ± 0.006
	1150.31	0.2860 ± 0.0014	147.475 ± 0.003
	1048.29	0.3110 ± 0.0031	148.413 ± 0.007
	947.16	0.3479 ± 0.0024	149.337 ± 0.003
	845.26	0.3884 ± 0.0062	150.262 ± 0.014
	744.26	0.4244 ± 0.0064	151.148 ± 0.009
	642.96	0.509 ± 0.027	152.026 ± 0.014
	524.86	0.636 ± 0.022	153.144 ± 0.035
300.00	2526.14	0.1530 ± 0.0018	148.302 ± 0.015
	2157.89	0.171 ± 0.023	150.604 ± 0.047
	1872.11	0.2107 ± 0.0061	152.436 ± 0.014
	1648.68	0.2374 ± 0.0053	153.859 ± 0.011
	1443.44	0.269 ± 0.011	155.168 ± 0.004
	1173.93	0.3247 ± 0.0090	156.882 ± 0.013
	975.51	0.404 ± 0.023	158.171 ± 0.028
	775.29	0.520 ± 0.033	159.49 ± 0.11
	581.57	0.742 ± 0.026	160.87 ± 0.10
	386.04	1.14 ± 0.72	161.89 ± 0.55
324.96	2540.96	0.1843 ± 0.0028	159.339 ± 0.004
	2322.23	0.1989 ± 0.0041	160.234 ± 0.013
	2114.40	0.2110 ± 0.0045	161.103 ± 0.004
	1936.20	0.2417 ± 0.0036	161.876 ± 0.010
	1769.00	0.2586 ± 0.0014	162.600 ± 0.005
	1487.57	0.3100 ± 0.0020	163.839 ± 0.013
	1257.38	0.360 ± 0.025	164.870 ± 0.023
	1070.79	0.422 ± 0.016	165.707 ± 0.016
	731.36	0.60 ± 0.22	167.213 ± 0.082
	582.54	0.884 ± 0.087	168.12 ± 0.22

TABLE 6
Kinematic viscosity v and speed of sound c of C_4F_8 at different temperatures

T/K	p/kPa	$10^6 v$/(m^2/s)	c/(m/s)
300.00	239.58	0.5545 ± 0.0050	107.039 ± 0.004
	209.45	0.6474 ± 0.0040	108.134 ± 0.011
	180.38	0.7621 ± 0.0068	109.165 ± 0.010
	160.13	0.8537 ± 0.0043	109.847 ± 0.005
310.00	359.99	0.421 ± 0.091	105.466 ± 0.091
	319.54	0.440 ± 0.015	106.837 ± 0.026
	259.63	0.545 ± 0.030	108.881 ± 0.017

TABLE 6 (*continued*)

T/K	p/kPa	$10^6 v$/(m^2/s)	c/(m/s)
	212.21	0.665 ± 0.077	110.435 ± 0.061
	167.11	1.04 ± 0.37	111.91 ± 0.16
315.00	410.27	0.3417 ± 0.0010	105.337 ± 0.005
	357.70	0.3988 ± 0.0026	107.159 ± 0.005
	312.27	0.4612 ± 0.0052	108.662 ± 0.004
	272.93	0.5380 ± 0.0097	109.919 ± 0.004
	234.75	0.639 ± 0.017	111.096 ± 0.013
	195.64	0.757 ± 0.021	112.234 ± 0.027
320.00	482.22	0.295 ± 0.013	104.314 ± 0.018
	380.03	0.3919 ± 0.0083	107.764 ± 0.019
	326.85	0.448 ± 0.015	109.445 ± 0.019
	274.43	0.538 ± 0.047	111.029 ± 0.045
	222.82	0.66 ± 0.12	112.465 ± 0.080
	172.92	0.92 ± 0.14	113.83 ± 0.17
	122.60	1.121 ± 0.076	115.18 ± 0.10
330.00	621.46	0.2365 ± 0.0022	103.148 ± 0.006
	536.09	0.2803 ± 0.0022	105.996 ± 0.005
	465.61	0.3296 ± 0.0017	108.183 ± 0.004
	376.53	0.4204 ± 0.0092	110.783 ± 0.005
	290.78	0.567 ± 0.066	113.105 ± 0.073
	215.35	0.777 ± 0.066	115.125 ± 0.045
330.00	621.46	0.2369 ± 0.0014	103.248 ± 0.003
	534.61	0.2827 ± 0.0021	106.126 ± 0.004
	450.70	0.3451 ± 0.0028	108.709 ± 0.003
	368.85	0.4301 ± 0.0055	111.063 ± 0.009
	288.39	0.563 ± 0.060	113.255 ± 0.021
	189.29	0.881 ± 0.041	115.790 ± 0.032
	117.49	1.433 ± 0.079	117.540 ± 0.086
345.04	881.89	0.1762 ± 0.0043	100.690 ± 0.004
	772.66	0.2056 ± 0.0026	104.173 ± 0.006
	652.37	0.2524 ± 0.0022	107.680 ± 0.002
	553.32	0.3045 ± 0.0015	110.349 ± 0.003
	445.79	0.386 ± 0.015	113.119 ± 0.067
	347.35	0.514 ± 0.010	115.420 ± 0.008
	244.86	0.730 ± 0.017	117.718 ± 0.020
360.00	1203.26	0.1354 ± 0.0030	97.726 ± 0.005
	1012.20	0.1684 ± 0.0029	103.467 ± 0.006
	802.73	0.2190 ± 0.0007	108.935 ± 0.007
	609.73	0.3202 ± 0.0211	113.456 ± 0.039
	407.30	0.474 ± 0.015	117.745 ± 0.012
	216.10	0.915 ± 0.022	121.468 ± 0.032
375.00	1620.38	0.1063 ± 0.0016	93.750 ± 0.006
	1402.03	0.1278 ± 0.0019	100.080 ± 0.012
	1188.17	0.1555 ± 0.0017	105.478 ± 0.007
	960.10	0.2046 ± 0.0032	110.614 ± 0.005
	758.63	0.259 ± 0.010	114.748 ± 0.025
	568.99	0.3537 ± 0.0035	118.340 ± 0.005
	378.87	0.553 ± 0.016	121.720 ± 0.009
	183.85	1.117 ± 0.034	124.967 ± 0.039

reported elsewhere [13]. In both cases, a very good agreement is found.

We only reported kinematic viscosity and speed of sound for the substances mentioned above; however, from c, it is possible to obtain a virial-type equation of state, and afterwards, it would be possible to derive η from the values of v reported here. This procedure will be exploited in a next paper.

TABLE 7
Kinematic viscosity v and speed of sound c of SF_6

T/K	p/kPa	$10^6 v/(m^2/s)$	c/(m/s)
273.16	1000.51	0.1808 ± 0.0022	111.810 ± 0.004
	903.28	0.224 ± 0.056	114.14 ± 0.08
	808.73	0.2352 ± 0.0008	116.211 ± 0.002
	712.29	0.2722 ± 0.0006	118.245 ± 0.001
	602.05	0.3283 ± 0.0012	120.453 ± 0.002
	492.40	0.4099 ± 0.0014	122.539 ± 0.004
	386.66	0.5327 ± 0.0006	124.461 ± 0.004
	290.38	0.7194 ± 0.0028	126.141 ± 0.001

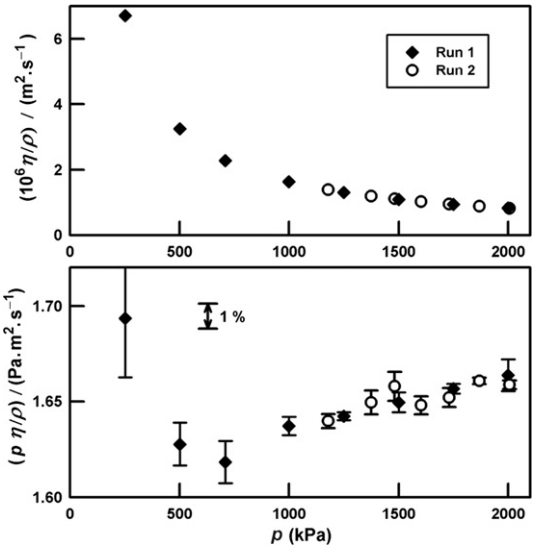

Figure 3. Reproducibility test of kinematic viscosity $v = \eta/\rho$. Top, two runs in CO at 300 K: run 1, ◆; run 2, ○. Bottom, $(p\eta/\rho)$ as function of p for the same two runs. Here error bars (one standard deviation) are visible and reproducibility is better than 1%.

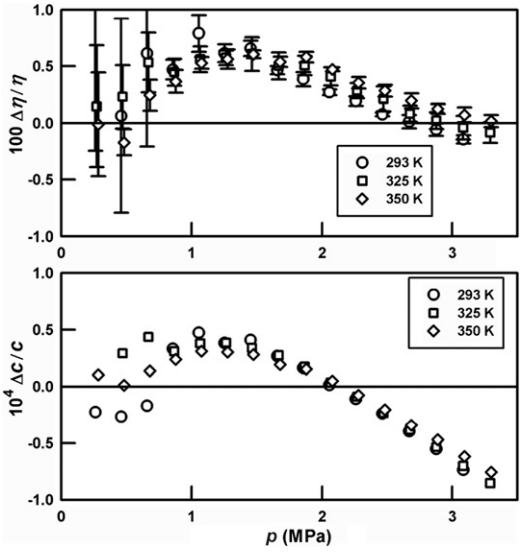

Figure 4. Performance of the Greenspan viscometer using Ar. Top; relative deviations of viscosity $\Delta\eta/\eta$ from values obtained from reference [1] at: 293.15 K, ○; 325 K, □; 350 K, △. Error bars are one standard deviation. Bottom; relative deviations of speed of sound $\Delta c/c$ from values obtained from reference [13] at: 293.15 K, ○; 325 K, □; 350 K, △.

5. Conclusions and summary

The network impedance model is a good representation of the Helmholtz resonance mode in our acoustic viscometer. The rounded edge design of this resonator allowed us to obtain a simple formula for end corrections as polynomial of the ratio δ_v/r_d. Geometry imperfections along the main duct and in the rest of the cavity demanded a calibration of the resonator with gases of known viscosity. We used an appropriated correction to the slit formed by the O-ring seal which works fine, but with a simple redesign of the two closures cap, we can get rid off this complication for good.

Then, after the calibration was completed, we obtain kinematic viscosity with a typical precision of about $\pm 0.3\%$, except at the low pressure end or when the resonance frequency is near a multiple of 60 Hz. However, the accuracy of our determinations is limited by the calibration therefore we estimated an overall uncertainty of about $\pm 0.6\%$ in the determination of kinematic viscosity. On the other hand, values of the speed of sound have a precision of few parts in thousand and the accuracy is about the same.

Acknowledgements

We thank Mike Moldover for his leadership, guidance and useful comments and James Mehl for his help modeling the physical acoustics.

References

[1] J. Wilhelm, E. Vogel, Int. J. Thermophys. 21 (2000) 301.
[2] C. Evers, H.W. Lösch, W. Wagner, Int. J. Thermophys. 23 (2002) 1411.
[3] R.F. Berg, Metrologia 42 (2005) 11.
[4] M. Greenspan, F.N. Wimenitz, An Acoustic Viscometer for Gases-I, NBS Report 2658 (1953).
[5] K.A. Gillis, J.B. Mehl, M.R. Moldover, Rev. Sci. Instrum. 67 (1996) 1850.
[6] J.B. Mehl, J. Acoust. Soc. Am. 106 (1999) 73.
[7] J. Wilhelm, K.A. Gillis, J.B. Mehl, M.R. Moldover, Int. J. Thermophys. 21 (2000) 983.
[8] K.A. Gillis, J.B. Mehl, M.R. Moldover, J. Acoust. Soc. Am. 114 (2003) 166.
[9] J.J. Hurly, K.A. Gillis, J.B. Mehl, M.R. Moldover, Int. J. Thermophys. 24 (2003) 1441.
[10] J.J. Hurly, Int. J. Thermophys. 25 (2004) 625.
[11] J.B. Mehl, private communication.
[12] J.B. Mehl, M.R. Moldover, L. Pitre, Metrologia 41 (2004) 295.
[13] A.F. Estrada-Alexanders, J.P.M. Trusler, J. Chem. Thermodyn. 27 (1995) 1075.
[14] J.J. Hurly, M.R. Moldover, J. Res. Natl. Inst. Stand. Technol. 105 (2000) 667.
[15] D. Seibt, E. Vogel, E. Bich, D. Butting, E. Hassel, J. Chem. Eng. Data 51 (2006) 526.
[16] P. Schley, M. Jaeschke, C. Küchenmeister, E. Vogel, Int. J. Thermophys. 25 (2004) 1623.
[17] J. Wilhelm, E. Vogel, J. Chem. Eng. Data 46 (2001) 1467.
[18] R. Span, E.W. Lemmon, R. T Jacobsen, W. Wagner, A. Yokozeki, J. Phys. Chem. Ref. Data 29 (2000) 1361.

[19] U. Setzmann, W. Wagner, J. Phys. Chem. Ref. Data 20 (1991) 1061.
[20] J.P.M. Trusler, M. Zarari, J. Chem. Thermodyn. 28 (1996) 329.
[21] E.W. Lemmon, M.O. McLinden, M.L. Huber, REFPROP, NIST Standard Reference Database, Version 7.0, Beta, version, 7/30/02. REFPROP is based on the most accurate pure fluid and mixture models currently available. It implements three models for the thermodynamic properties of pure fluids: equations of state explicit in Helmholtz energy, the modified Benedict–Webb–Rubin equation of state, and an extended corresponding states (ECS) model. Mixture calculations employ a model which applies mixing rules applied to the Helmholtz energy of the mixture components; it uses a departure function to account for the departure from ideal mixing. Viscosity and thermal conductivity are modeled with either fluid-specific correlations or an ECS method.

JCT 07-118